

Effect of Lubricant Contamination on EHL Rolling Contact: Response Surface Methodology

Sabrina MAATALLAH¹⁾, Mohamed Rafik SARI^{1, 2)},
Lakhdar KHOCHEMANE¹⁾

¹⁾ *University of Skikda*
Mechanical Engineering Department
El Hadaiek Road, B. O. 26, 21000 Skikda, Algeria
e-mail: sari_rafik10@yahoo.fr

²⁾ *University Badji Mokhtar of Annaba*
Industrial Mechanics Laboratory
B. O. 12, 23000 Annaba, Algeria

In this research the failure of EHL rolling contact in highly contaminated media is investigated. The conducted study uses an original experimental device to predict the effects of operating parameters, namely, surface hardness, contaminant concentration, rotational velocity, and the applied load on wear and roughness components. The planning of the experiments was based on Taguchi's L_9 orthogonal array. The statistical significance of the above mentioned parameters on the results was explored using the analysis of variance (ANOVA). The relationship between responses' factors and the operating parameters is also established employing the multiple linear regression method. ANOVA results show clearly that the surface hardness (H) and contaminant concentration (C) are the most significant factors that influence wear and surface roughness of machine elements.

Key words: rolling contact, lubricant contamination, wear, roughness, response surface methodology.

1. INTRODUCTION

Nowadays, it is well known that the presence of solid particles in lubricant oil can have dramatic consequences. In contaminated environments, like the Sahara, sand concentration in the air is very high (15–35 mg/m³), and it is 10–100 times higher in the presence of wind. Dust particles carried by wind have various sizes going from smaller than a micron to a few millimeters. Consequently, these undesirable particles can damage surfaces and lead to fatigue and wear of machine components.

To reduce the injurious effects of solid particles, the lubricant is usually filtered; however, filtration does not eliminate the contact of particles with the surfaces because very fine particles could pass through the filter meshes. In fact, when their size is larger than the oil film thickness ranging from 0.1 to 1 μm , they dent the surface and cause severe wear, thus leading to the fast failure of mechanisms.

Over the last decades, the effect of solid contamination of lubrication has received much attention and was studied intensively by many authors. According to the literature, numerous numerical and experimental studies dealing with the effect of lubricant contamination on an EHL contact have been performed. Also, it is worth noting that the majority of experimental contributions use a smooth ball-plane device where the ball is given a rotational movement on a glass disk. WEDEVEN and CUSANO [1, 2] and KANETA *et al.* [3–5] have used this test rig to follow the evolution of an artificial dent during operating cycles and its influence on the oil film thickness.

By theoretical means, many authors [6–11] calculated the pressure field in the presence of a single dent on the surfaces. KANG *et al.* [12] also showed the evolution of pressure field and oil film thickness in an EHL contact under the effect of solid particles.

Based on particles of various sizes and characteristics, DWYER JOYCE [13] classified particles (ductile, brittle, and ceramics hard) according to their behavior in the contact. CANN *et al.* [14] undertook a study on the deformation of particles in the contact by using an optical interferometer technique. The adopted technique gives a direct measurement of the size of the dents produced and allows the calculation of the pressure caused by particles. VILLE and NELIAS [15] in their experimental study showed the effect of spherical ductile metal particles in an EHL contact. WAN and SPIKES [16] established a classification of particles according to their behaviour with surfaces' contact. This study is mainly based on the impact of hard ceramic particles as compared to the effect of ductile particles. JIN and YANG [17], by a ferrographic analysis applied to the condition monitoring of locomotive engines, gave an overall picture of particles generated in such types of engines. AKAGAKI *et al.* [18] studied friction and wear behaviours of rolling bearing lubricated in contaminated oil containing white-fused alumina particles. PENG *et al.* [19] established a correlation between vibration and wear debris analysis. This study gives more understanding on diagnosing machine faults. Based on imaging technology for shape and composition detection, KHAN *et al.* [20] presented a new methodology for online wear debris shape and composition analysis. In a previous work [21], SARI *et al.* studied the effect of lubricant contamination on gear wear. They showed that the presence of very fine sand particles in lubricant oil leads to significant wear in the first few operating cycles at the level of the tooth root. SARI *et al.* [22] also showed that

the presence of solid particles in the lubricant oil disturbs the proper operation of the oil film leading to noticeable fluctuations of film thickness and higher friction coefficient.

To our knowledge, no statistical study devoted to the development of empirical models dealing with the effect of operating parameters on the evolution of wear and surface roughness in highly contaminated media has been done yet. In fact, this research uses an original experimental device to investigate the effect of solid contamination of lubrication on the evolution of wear and temperature in an EHL rolling contact. On the other hand, the response surface methodology (RSM) and analysis of variance (ANOVA) were used to develop statistical models for wear (W) and roughness components (R_a and R_t), and to predict the effects of surface hardness, contaminant concentration, rotational speed, and the applied load on the responses of interest.

2. EXPERIMENTATION

2.1. Experimental device

To show the effect of solid contamination of lubrication on the failure of EHL rolling contact, an original experimental test rig (Fig. 1) was built. In fact, the used test rig was designed for the investigation of two disks' contacts.

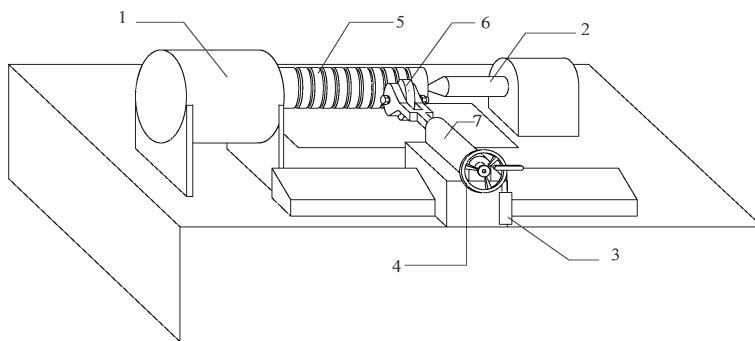


FIG. 1. Schematic diagram of experimental device: 1 – electrical motor, 2 – rotary live center, 3 – loads, 4 – manual lever, 5 – steel cylindrical specimen, 6 – rotary steel disk, 7 – transverse carriage.

The principle is to put in contact a steel disk with a steel cylindrical sample. As shown in Fig. 1, the used cylindrical sample is in the form of round bars with a 30 mm diameter and 240 mm length. The cylindrical sample contains many bands considered as disks. On the other hand, the considered disks are connected with sub-category C45. In this study, we use only one type of material. Table 1 shows the mechanical and geometrical properties of the steel disks.

Table 1. Mechanical and geometrical properties of steel disks.

Characteristics	Steel disk	Cylindrical specimen 1	Cylindrical specimen 2	Cylindrical specimen 3
Diameter [mm]	30	30	30	30
Length, L_1 [mm]	—	240	240	240
Materials	C45	C45	C45	C45
Hardness HRC	34	46	55	59
Poisson coefficient ν	0.3	0.3	0.3	0.3
Young modulus E [GPa]	210	210	210	210
Initial roughness R_a [μm]	0.2	0.2	0.2	0.2
Initial roughness R_t [μm]	1.3	1.3	1.3	1.3
Radius of relative curvature R_x [mm]	15	15	15	15
Face width of contact L [mm]			12	

In order to maintain a constant meniscus of lubricant oil between disks, we use a feed gravity system (Fig. 2).

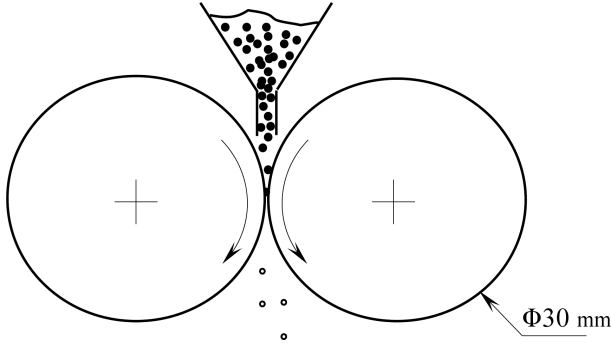


FIG. 2. Rolling contact model.

In this study, the wear of steel disks is evaluated by diametral loss using a digital calliper. The temperature was evaluated at the contact point. An infrared thermocouple was used for the temperature measurements. For roughness measurements (R_a and R_t), a roughness tester MITUTYO surftest 301 was used and the measurements were taken at three locations around the circumference of the cylindrical bands. Results are an average of the obtained values. Hardness measurements of the cylindrical specimen were carried out using a hardness tester Mitutoyo HH-401. The principle consists of indenting the steel cylindrical specimen with a diamond cone indenter. Measurements were reproduced at five equally spaced locations along the cylindrical specimen. The average value was considered.

2.2. Calibration procedure

Firstly, the rotary disk is moved linearly, while the cylindrical specimen rotates. Indeed, when a tangent between the two disks is provided, we stop immediately the electrical motor.

Thereafter, we proceed to calibration in order to determine the load between disks. The principle of calibration is given as follows:

On the opposite face of the contacting surfaces, we place a mechanical dial gauge which is adjusted to zero. Then, several loads are suspended on the manual lever. Consequently, the transverse carriage moves. Under the loads action, the steel disk presses the cylindrical specimen. For each cylindrical band, we have established a calibration graph. In fact, the deformation of each band (Y_1) is measured. In this situation, the cylindrical specimen is considered as a beam with fixed ends (see Fig. 3).

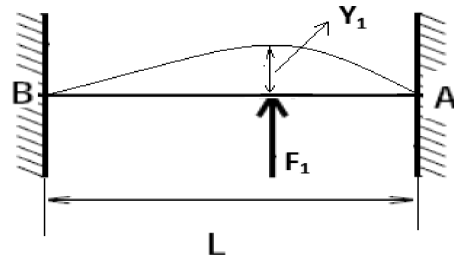


FIG. 3. Applied load on the cylindrical specimen.

The deformation (Y_1) of each cylindrical band is measured by a mechanical dial gauge and results are reported in Table 2.

Table 2. Deformation values of C45 steel cylindrical specimen for each cylindrical band.

Load Q [Kg]	Load F_1 [N]	Y_1 [mm]								
		Cylindrical band 1	Cylindrical band 2	Cylindrical band 3	Cylindrical band 4	Cylindrical band 5	Cylindrical band 6	Cylindrical band 7	Cylindrical band 8	Cylindrical band 9
1	9.81	0.005	0.008	0.01	0.015	0.025	0.02	0.015	0.01	0.01
2	19.62	0.02	0.042	0.045	0.05	0.055	0.05	0.04	0.03	0.015
4	39.24	0.06	0.07	0.1	0.09	0.09	0.08	0.08	0.07	0.065
5	49.05	0.07	0.1	0.13	0.14	0.12	0.12	0.12	0.1	0.07
8	78.48	0.12	0.14	0.16	0.17	0.18	0.17	0.15	0.13	0.13
12	117.72	0.15	0.21	0.27	0.28	0.29	0.27	0.25	0.2	0.15

On the other hand, for the calibration graphs of cylindrical bands, a perfect linear relationship between Y_1 and F_1 is observed. As displayed in Fig. 4, the calibration graphs are linear and have the following form:

$$(2.1) \quad Y_i = K \cdot F_{1i},$$

where Y is the predicted deformation, F_1 is the applied load, and K is the calibration constant.

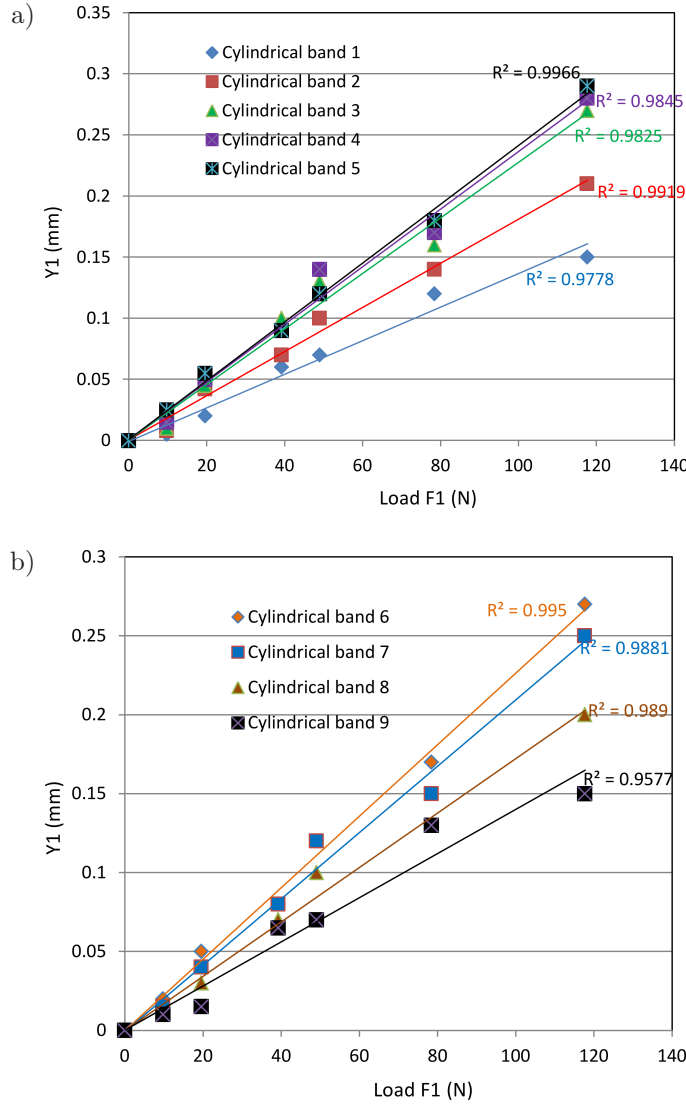


FIG. 4. Applied load on the cylindrical specimen: a) cylindrical bands 1 to 5, b) cylindrical bands 6 to 9.

To calculate the calibration constant K , we apply the least squares method. This method is a procedure to determine the best fit line to data. For example, the calculation of calibration constant of the cylindrical band 5 is given as follows:

Consider the squares sum of differences (error) between the experimental values Y_1 and those of the predicted Y function:

$$(2.2) \quad Z = \sum_{i=1}^6 (Y_{1i} - Y_i)^2.$$

The goal is to find values of K that minimize the error. In fact, these values are given as follows:

$$(2.3) \quad \frac{\partial Z}{\partial K} = 0.$$

Operating with (2.3), we obtain:

$$(2.4) \quad \frac{\partial Z}{\partial K} = 2 \sum_{i=1}^6 [K \cdot F_{1i}^2 - Y_{1i} \cdot F_{1i}],$$

$$(2.5) \quad \frac{\partial Z}{\partial K} = 0 - \sum_{i=1}^6 Y_{1i} \cdot (F_{1i}) + \sum_{i=1}^6 K \cdot F_{1i}^2 = 0.$$

According to Eq. (2.5), we find:

$$(2.6) \quad K = \frac{\sum_{i=1}^6 Y_{1i} \cdot F_{1i}}{\sum_{i=1}^6 F_{1i}^2}.$$

Operating with the data of cylindrical band 5 in Table 2, Eq. (2.6) yields:

$$K = 0.00241398.$$

The contact force (real applied load) between steel disks is given as follows:

$$(2.7) \quad F_1 = \frac{1}{K} \cdot Y_1 = \frac{1}{0.00241398} \cdot Y_1 = 414.254364 \cdot Y_1.$$

Finally, in Table 3 the results of the calibration constant [1/K] for all studied cylindrical bands are gathered.

Table 3. Calibration constant of cylindrical bands.

Cylindrical band	Constant [1/K]
1	733.944035
2	552.24734
3	439.460317
4	422.687023
5	414.254364
6	441.797872
7	477.802493
8	580.825175
9	713.965616

2.3. Lubricant

The lubricant used is ISO VG 220 oil. It has a dynamic viscosity $\mu_0 = 0.033 \text{ Pa}\cdot\text{s}$ at $T_0 = 40^\circ\text{C}$ and a piezo-viscosity coefficient $\alpha_{pv} = 18.2 \cdot 10^{-9} \text{ Pa}^{-1}$. It is representative of transmission oil, and is often used for gears greasing by splashing and circulation.

2.4. Contaminant

The used contaminant is desert sand which can be conveyed by the wind as far as Europe and even America. It is very rich in silica, with 90% of quartz. It was cleaned, filtered to 63 μm , and analysed chemically. The chemical constitution and morphology of sand particles are given in (Fig. 5).

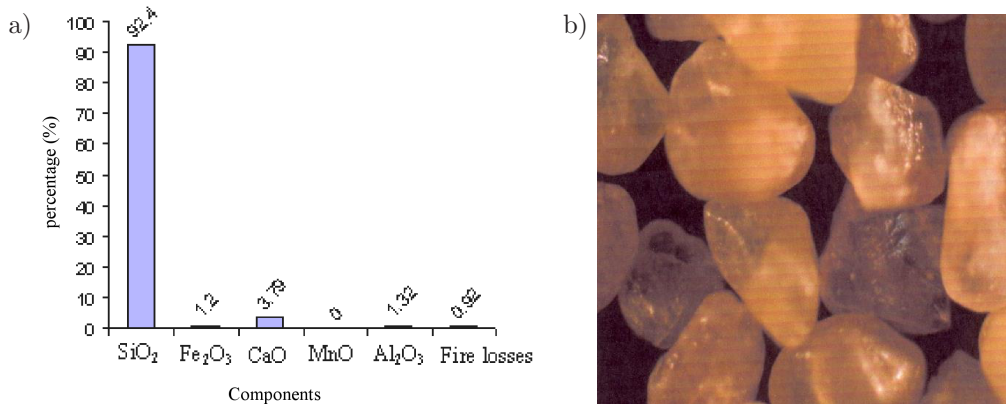


FIG. 5. Chemical constitution and morphology of sand particles: a) chemical constitution, b) sand particles morphology.

3. DESIGN OF EXPERIMENTS

Taguchi method was developed by Dr. Genichi Taguchi since 1960s in order to enhance the quality of manufactured products. Thereafter, this robust statistical method has attracted the attention of researchers' community. In fact, Taguchi method was intensively applied to a wide research activity such as: engineering, biotechnology, and marketing.

Taguchi method is an experimental design technique that allows obtaining significant factors at low cost and a reduced number of experiments by using orthogonal arrays. On the other hand, the design factors could easily produce the best levels of measure.

In this research, the data used for computation have been obtained by designing the experiments based on Taguchi L_9 orthogonal array. Each input variable is varied according to three levels coded as 1, 2, and 3. The levels of the input variables (i.e., surface hardness of the cylindrical specimen (H), contaminant concentration (C), rotational speed (V), and the applied load (Q)) are displayed in Table 4. On the other hand, following the Taguchi technique, the experiments' design consists of 9 runs as presented in Table 5.

Table 4. Assignment of the factor levels.

Level	Hardness H (HRC)	Contaminant concentration C [g/l]	Applied load Q [Kg]	Rotational speed V [rpm]
1	46	5	10	200
2	55	7.5	13	400
3	59	10	16	640

Table 5. Wear and roughness results for various combinations of operating parameters.

Test	Coded Factors				Actual Factors				Responses' Factors		
	X_1	X_2	X_3	X_4	H (HRC)	C [g/l]	Q [Kg]	V [rpm]	W [mm]	R_a [μm]	R_t [μm]
1	1	1	1	1	46	5	10	200	0.092	0.65333	8.5
2	1	2	2	2	46	7.5	13	400	0.109	0.82333	11.6
3	1	3	3	3	46	10	16	640	0.11	1.26333	12
4	2	1	2	3	55	5	13	640	0.062	0.52133	6.7333
5	2	2	3	1	55	7.5	16	200	0.066	0.55667	6.9667
6	2	3	1	2	55	10	10	400	0.0904	0.72667	7.6333
7	3	1	3	2	59	5	16	400	0.058	0.39333	3.3333
8	3	2	1	3	59	7.5	10	640	0.06	0.44667	5.8667
9	3	3	2	1	59	10	13	200	0.088	0.70667	7.9667

In the present research, the relationship between the four input variables (H , C , V , and Q) and the output parameters yy which define the responses factors (wear (W) or roughness parameters (R_a and R_t)) is given as follows:

$$(3.1) \quad yy = f(H, C, Q, V).$$

The relationship (3.1) can be approximated by the following linear mathematical model:

$$(3.2) \quad yy = b_0 + \sum_{i=1}^k b_i \cdot X_i,$$

where b_0 is the free term of the model equation, b_1, b_2, \dots, b_k are the linear terms, and X_i represents input parameters (H , C , V , and Q).

4. RESULTS AND DISCUSSIONS

Figure 6 displays the wear evolution versus operating time for a contact force $F_1 \cong 180$ N and rotational velocity $V = 250$ rpm. The contact between cylindrical disks is linear. In fact, using data of Table 1, the maximum hertzian pressure P_0 , for a linear contact is calculated by:

$$P_0 = \frac{2F_1}{\pi a L} \cong 192 \text{ MPa},$$

where a is contact half-width, $a = \left[\frac{8 \cdot F_1 \cdot R_x}{\pi \cdot L \cdot E'} \right]^{1/2} = 4.982 \cdot 10^{-5}$ m, E' is equivalent Young modulus, $E' = \left[\frac{1}{2} \cdot \left(\frac{1-\nu_1^2}{E_1} + \frac{1-\nu_2^2}{E_2} \right) \right]^{-1} = 230.76$ GPa.

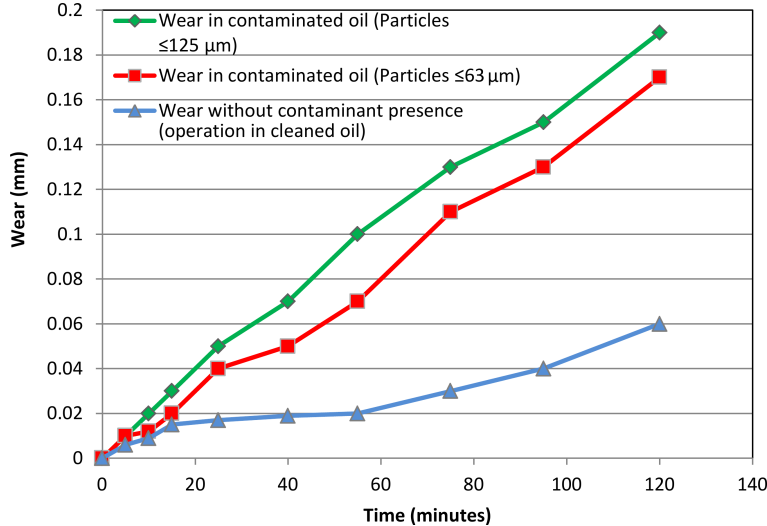


FIG. 6. Effect of lubricant contamination on the evolution of surface wear.

According to Fig. 6, an increase on wear was observed for both operations without and with the presence of sand particles. In contaminated media, the increase in wear is mainly caused by the presence of sand particles in the lubricant oil, in addition to the wear debris generated during the operation. On the other hand, it can be also seen that the presence of large solid particles ($d \leq 125 \mu\text{m}$) in the lubricant disturbs the oil film thickness, rises the friction between the contacting surfaces, and consequently the wear is relatively higher from that observed for other operating conditions.

The mechanical energy lost by friction is generally transformed into heat. In fact, this heating is sometimes very difficult to evacuate. The thermal aspects of friction can have unexpected consequences. As depicted in Fig. 7, we observe that the temperature rises during the first operations cycles, then is stabilized. This heating comes from elastic and plastic deformations, repeating itself at high speed and mainly accompanied by sliding and frictional stress. The increasing temperature is accentuated with the presence of solid particles in the lubricant oil. This can be explained by the increase of friction for the operation in a contaminated oil.

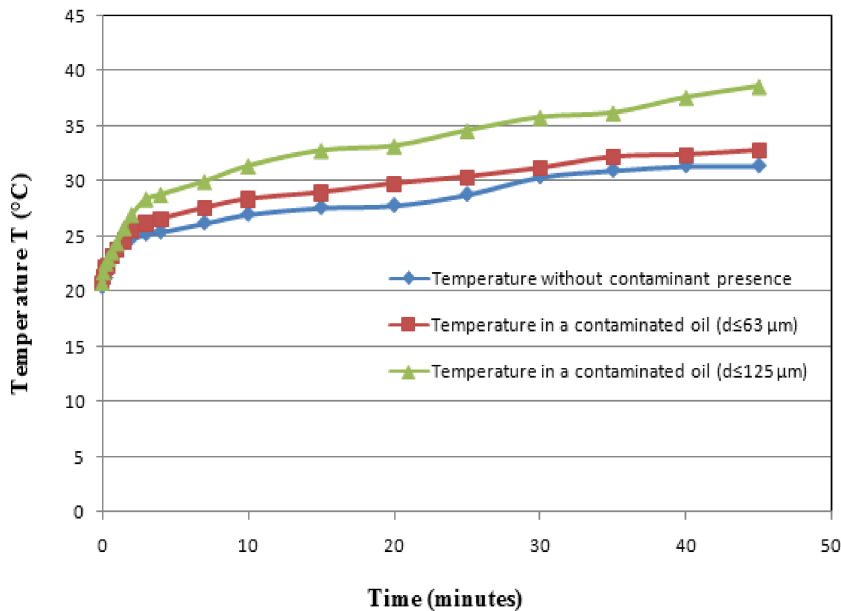


FIG. 7. Effect of lubricant contamination on the temperature evolution.

Figure 8 shows the micrograph of steel disk surface before the operation. Figure 9 depict the micrograph of worn surfaces of the EHL rolling contact after the operation in a clean and contaminated oil respectively. It can be observed

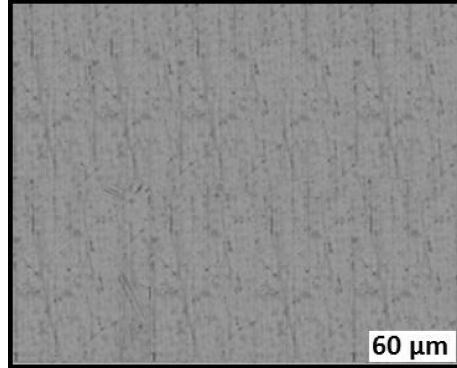
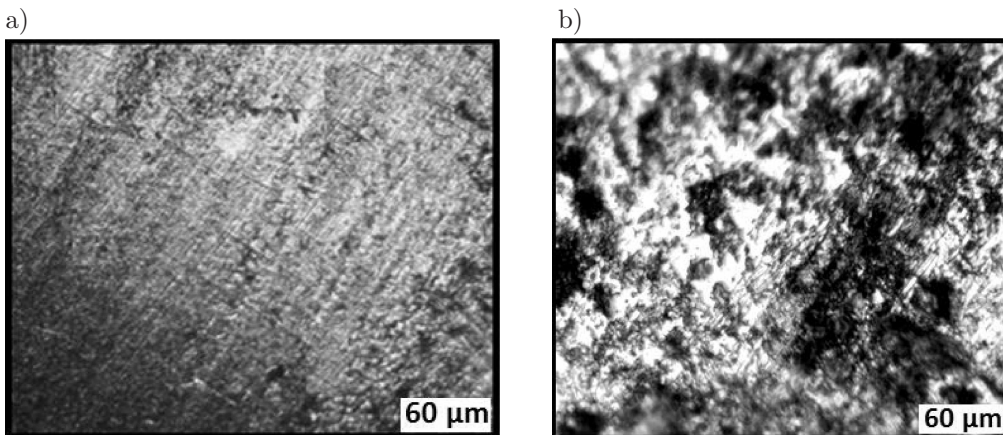


FIG. 8. Steel disk aspect before operation.

FIG. 9. Optical micrograph of a steel disk after the operation in: a) a cleaned oil ($F_1 = 180$ N and $V = 250$ rpm), b) a contaminated oil (particles ≤ 125 μm , $C = 5$ g/l, $F_1 = 180$ N and $V = 250$ rpm).

from the micrograph that the wear is very smooth for the operation in the cleaned oil (Fig. 9a); however, as displayed in Fig. 9b, the wear is very severe for the operation in the contaminated oil. In this last case, the presence of sand particles in the lubricant oil accelerates the degradation and the observed wear is mainly associated with adhesion and indentation. In the rolling contact, the presence of dent in the surface is worthy and constitutes undoubtedly a specific site of fatigue.

According to the experimental results presented in Table 5, regression equations were developed using the multiple regression method. These models are considered as linear functions of the surface hardness (H), contaminant concentration (C), rotational velocity (V), and the applied load (Q). The regres-

sion equations of the fitted models for wear (W) and roughness parameters (Ra and Rt) are expressed as follows:

$$(4.1) \quad W = 0.205 - 0.00282H + 0.00509C - 0.000047Q - 0.000011V,$$

$$(4.2) \quad Ra = 1.40086 - 0.031282H + 0.0752453C + 0.00214811Q + 0.000243707V,$$

$$(4.3) \quad Rt = 23.2841 - 0.385588H + 0.602227C + 0.00166667Q + 0.000947756V,$$

where W is the surface wear in mm, H is the hardness of the cylindrical specimen in HRC, C is the contaminant concentration in g/l, Q is the applied load in Kg, V is the rotational speed in rpm, Ra is the arithmetic mean roughness in μm , and Rt is the peak-to-valley height roughness in μm .

In order to compare the predicted values of response factors governing wear (W) and surface roughness components (Ra and Rt) to the experimental data, the coefficient of determination (R^2) was calculated. Indeed, when R^2 (R -squared) approaches unity (Table 6), the predicted values and experimental data are in an excellent agreement. As depicted in Figs. 10–12, the obtained results also justify the validity, applicability, and good accuracy of the obtained regression equations for wear (W) and surface roughness components (Ra and Rt) when compared to the experimental values.

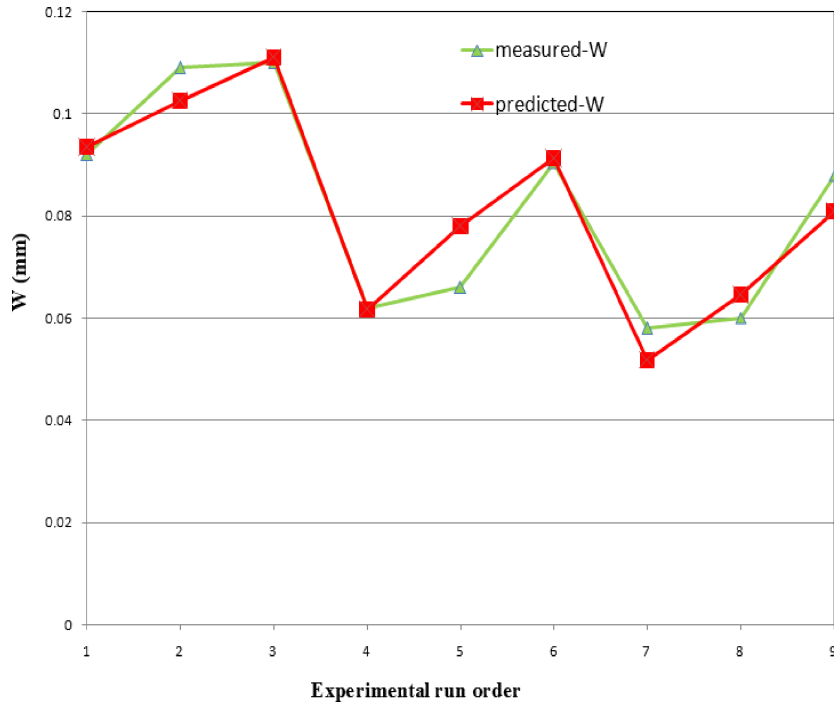


FIG. 10. Comparison between the measured and predicted values for wear.

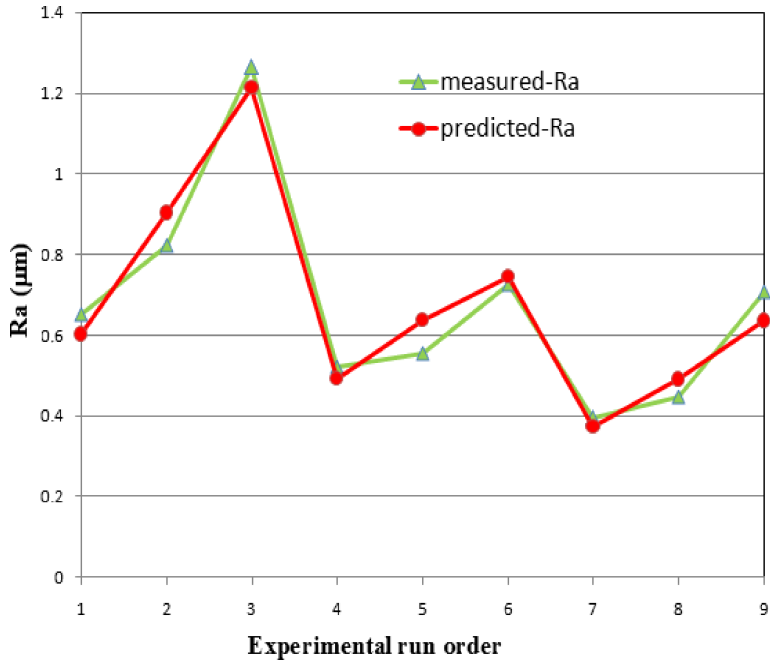


FIG. 11. Comparison between the measured and predicted values for surface roughness R_a .

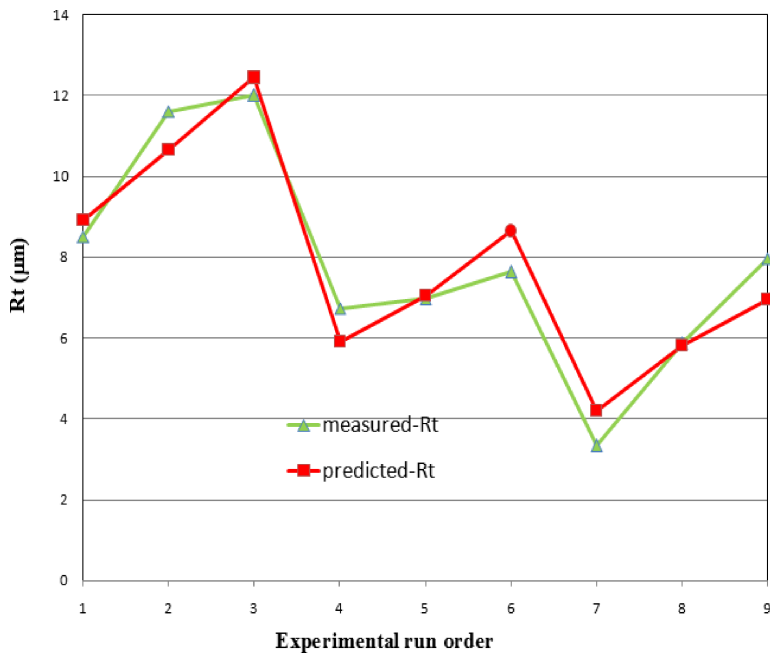


FIG. 12. Comparison between the measured and predicted values for surface roughness R_t .

Table 6. Coefficient of determination.

Model	Coefficient of determination R^2
Wear W	0.9123
Roughness R_a	0.951
Roughness R_t	0.9191

A variance analysis (ANOVA) of wear (W) and surface roughness parameters (R_a and R_t) was investigated. The principal goal of this analysis is to investigate the effects of the input parameters, i.e., hardness (H), contaminant concentration (C), rotational speed (V), and the applied load (Q), on the studied responses. Due to conducting the experiments according to the Taguchi orthogonal array, results for various combinations of the input parameters were depicted in Table 5. It is worth noting that the analysis of the variance (ANOVA) is carried out for the level of significance of 5% (i.e., the level of confidence 95%). ANOVA results for W , R_a , and R_t are displayed in Tables 7–9. In fact, these tables show the degrees of freedom (DF), sum of squares (SS), mean square (MS),

Table 7. ANOVA results for wear (W).

Source	DF	SS	MS	F-value	Prob.	Pc [%]
Regression	4	0.0031335	0.0007834	10.3983	0.021741	—
H	1	0.0021109	0.0021109	28.0198	0.006115	66.72
C	1	0.0009728	0.0009728	12.9131	0.022891	30.75
Q	1	0.0000118	0.0000118	0.1561	0.712936	0.37
V	1	0.000038	0.000038	0.5041	0.516923	1.20
Error	4	0.00003013	0.0000753	—	—	0.95
Total	8	0.0034348	—	—	—	—

Table 8. ANOVA results for surface roughness (R_a).

Source	DF	SS	MS	F-value	Prob.	Pc [%]
Regression	4	0.514831	0.514831	19.4238	0.006957	—
H	1	0.260298	0.260298	39.2827	0.003307	48.08
C	1	0.21232	0.21232	32.0421	0.004801	39.22
Q	1	0.024918	0.024918	3.6704	0.124494	4.60
V	1	0.017295	0.017295	2.6101	0.181488	3.19
Error	4	0.026505	0.006626	—	—	4.89
Total	8	0.541336	—	—	—	—

Table 9. ANOVA results for surface roughness (R_t).

Source	DF	SS	MS	F-value	Prob.	Pc [%]
Regression	4	53.4254	13.3564	11.3582	0.018583	–
H	1	39.5485	39.5485	33.632	0.004397	68.03
C	1	13.6004	13.6004	11.5658	0.027256	23.39
Q	1	0.015	0.015	0.0128	0.915518	0.026
V	1	0.2616	0.2616	0.2224	0.661764	0.45
Error	4	4.7037	4.7037	–	–	8.09
Total	8	58.1291	–	–	–	–

F-values (F-val.), and probability (Prob.). A low probability (Prob. < 0.05) indicates the statistical significance of the source factor for the corresponding response.

The percentage contribution (Pc %) of each input variable on the total variation of responses was also calculated and reported in the last columns of Tables 7–9. In fact, it gives the degree of influence of each variable on the results.

According to the results depicted in Table 7, we notice that the surface hardness ($Pc = 66.2\%$) and contaminant concentration ($Pc = 30.75\%$) have a great effect on the wear evolution. In fact, the presence of sand particles in the lubricant oil with a decrease of surface hardness accelerates the failure and leads to an increase in the wear. On the other hand, the load (Q) and rotational speed (V) do not have significant effect on the wear. Respectively, their contributions are 0.37% and 1.2%.

From Table 8, it is also well observed that the surface hardness and contaminant concentration have a bigger effect, which explains 48.08% and 39.22% on the total variability of the arithmetic mean of the surface roughness R_a . The load, Q and rotational speed, V , are not significant because their contributions are 4.6% and 3.19%, respectively.

As shown in Table 9 for maximum peak-to-valley height (R_t), the analysis of the variance shows that the surface hardness (H) is the most significant factor influencing R_t . Its contribution is 68.03%. The second factor affecting R_t is the contaminant concentration with 23.39%. It is also seen that the load Q and rotational speed V do not have any statistical influence with 0.026% and 0.45% contributions, respectively.

Figures 13–15 give the main factor effects on wear and surface roughness. It is clearly shown that wear W and the surface roughness components (R_a and R_t) are decreasing functions of the surface hardness H , while their behaviour is quite different as compared to the contaminant concentration C . In fact, they are increasing functions of the contaminant concentration C . On the other hand,

it is also noticed that the load Q and rotational speed V have little effect on the obtained results.

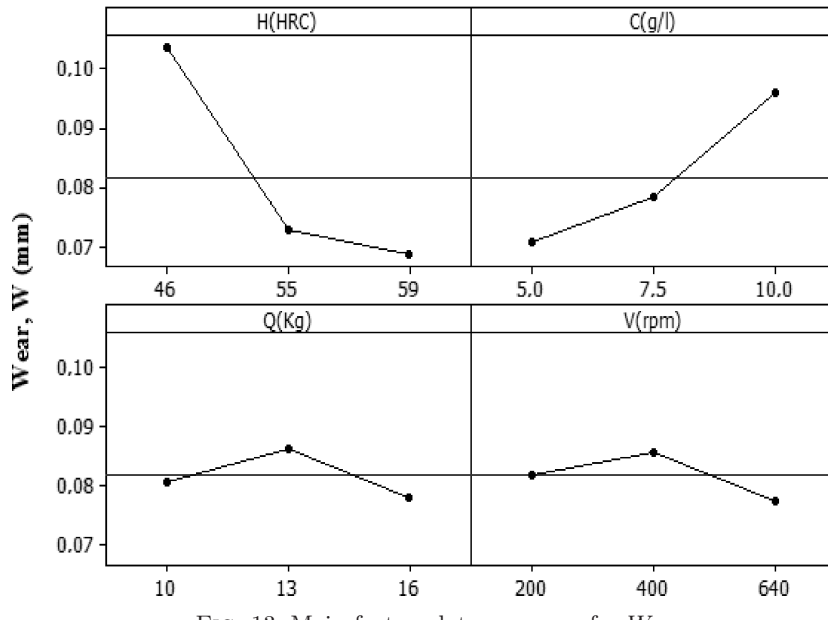


FIG. 13. Main factor plots: averages for W .

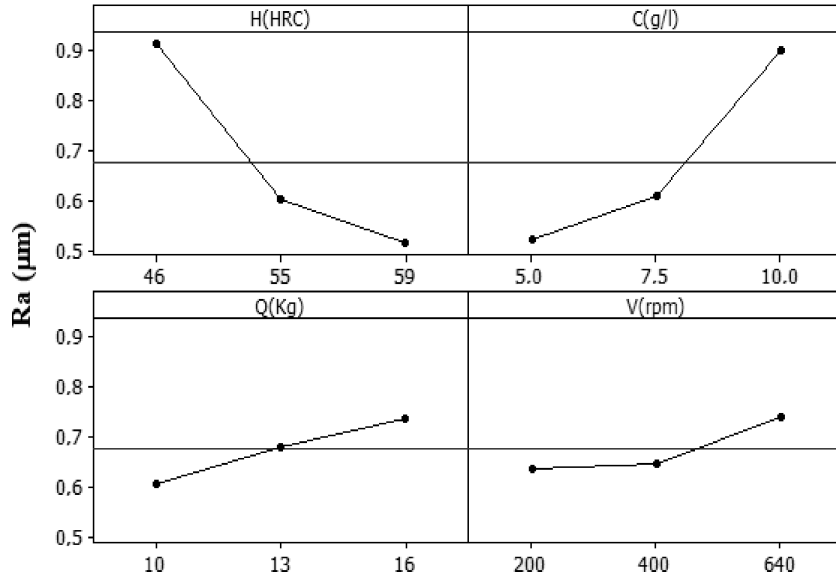
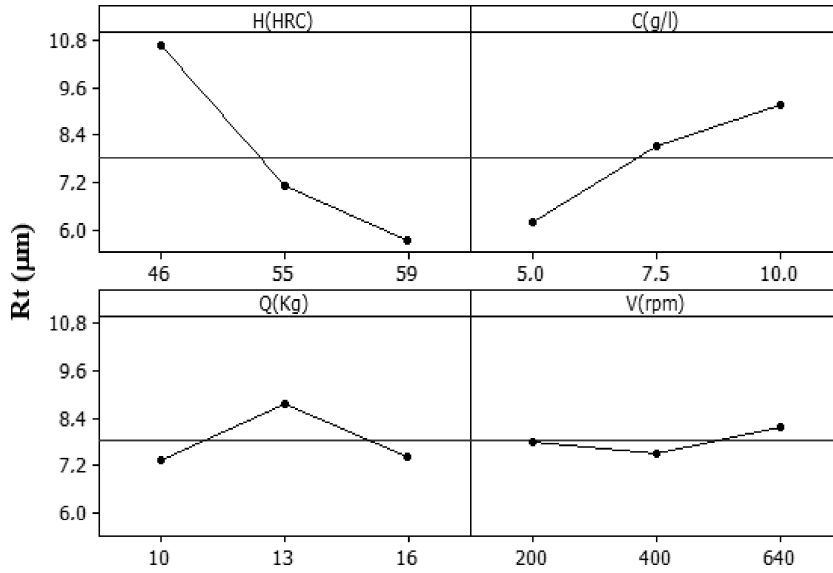


FIG. 14. Main factor plots: averages for R_a .

FIG. 15. Main factor plots: averages for Rt .

5. CONCLUDING REMARKS

This study deals with the effect of operating parameters on surfaces' degradation in relationship to the presence of solid contaminants in the lubricant oil. To achieve this goal, an original experimental device that simulates real operating conditions of a rolling EHL contact was built and then successfully used to follow the degradation of surfaces' contact. On the other hand, mathematical models for wear (W) and roughness components (Ra and Rt) were developed by the application of response surface methodology. The obtained models show the effect of the operating parameters, i.e., hardness (H), contaminant concentration (C), rotational speed (V), and the applied load (Q), on the studied responses.

The principal conclusions which we can draw from this study are summarized as follows:

- The presence of solid particles in the lubricant oil raises friction and causes a notable wear in the first operational cycles. Consequently, the temperature between the contacting surfaces increases.
- From the optical micrograph, it is highly noticed that the wear is very smooth in a cleaned oil; however, it is connected with adhesion and indentation for operation in a contaminated oil.
- The wear (W) and roughness components (Ra and Rt) decrease with the increase of the cylindrical specimen hardness (H) and increase with the increase of the contaminant concentration (C).

- This investigation uses L_9 orthogonal array for four designing parameters which are: surface hardness, rotational speed, contaminant concentration, and the applied load. In fact, nine experiments were established instead of the total factorial 81 experiments. As a result, Taguchi method allows obtaining significant factors at a low cost, short experimental time, and a reduced number of experiments.
- The response surface methodology (RSM) is a very useful tool that gives predicting models for responses' factors in highly contaminated media.
- ANOVA results show that the surface hardness (H) and contaminant concentration (C) are the factors which have a higher effect on the evolution of wear and surface roughness.
- The comparison of both the experimental and predicted values shows a good agreement between the results.
- Finally, the main question that arises from this study is how to determine the real applied force with a high precision. It is also well established that the load is directly proportional to the real area of contact between contacting surfaces. In fact, the load is not stable during the wear process and decreases with a decrease of the contact area. With this intent, we will try in a future work to establish the correlation between the load and produced wear. Consequently, we can predict with precision the variation of load during the wear process.

REFERENCES

1. CUSANO C., WEDEVEN L.D., *The influence of surface dents and grooves on traction in sliding EHD point contacts*, ASLE Transactions, **26**(3): 306–310, 1982.
2. WEDEVEN L.D., CUSANO C., *Elastohydrodynamic film thickness measurements of artificially produced surface dents and groove*, ASLE Transactions, **22**(4): 369–381, 1979.
3. KANETA M., SAKAI T., NISHIKAWA H., *Optical interferometric observations of the effects of a bump on point contact EHL*, ASME Journal of Tribology, **114**(4): 779–784, 1992.
4. KANETA M., NISHIKAWA H., *Local reduction in thickness of point contact EHL films caused by a transversely oriented moving groove and its recovery*, ASME Journal of Tribology, **116**: 635–639, 1994.
5. KANETA M., KANADA T., NISHIKAWA H., *Optical interferometric observations of the effects of a moving dent on point contact*, Tribology Series, **32**: 69–79, 1997.
6. KO C.N., IOANNIDES E., *Debris denting – The associated residual stresses and their effect on the fatigue life of sliding bearing, an FEM analysis*, Proceedings of 15th Leeds-Lyon Symposium on Tribology, Elsevier, Amsterdam, 199–207, 1989.
7. LUBRECHET A.A., VANNER C.H., LANE S., JACOBSON B., IOANNIDES E., *Surface damage – comparison of theoretical and experimental endurance lives of rolling bearings*, Proceedings of the Japan International Tribology Conference, Nagoya, Japan, 185–190, 1990.

8. LUBRECHT A.A., DWYER-JOYCE R.S., IOANNIDES E., *Analysis of the influence of indentations on contact life*, Tribology Series, **21**: 173–181, 1992.
9. AI X., CHENG H.S., *The influence of moving dent on point EHL contacts*, STLE Tribology Transactions, **37**: 323–335, 1994.
10. NIXON H.P., ZANTOPULOS H., *Fatigue life performance – Compared of tapered roller bearing with debris dam-aged raceways*, Lubrication Engineering, **5**(19): 732–736, 1995.
11. AI X., LEE S.C., *Effect of slide to roll ratio on interior stresses around a dent in EHL contacts*, STLE Tribology Transactions, **39**(4): 881–889, 1996.
12. KANG Y.S., SADEGHI F., AI X., *Debris effect on EHL contact*, ASME Journal of Tribology, **122**(4): 711–720, 2000.
13. DWYER JOYCE R.S., HAMER J.C., SAYLES R.S., IOANNIDES E., *Surface damage effects caused by debris in rolling bearing lubricants, with an emphasis on friable materials. rolling element bearings*, Mechanical Engineering Publications for the I. Mech. E., 17–24, 1990
14. CANN P.M.E., HAMER J.C., SAYLES R.S., SPIKES H.A., IOANNIDES E., *Direct observation of particle entry and deformation in rolling EHD contact*, [in:] Dowson D. et al. [Eds.], Proceedings of 22nd Leeds-Lyon Symposium on Tribology, Elsevier, Amsterdam, 127–134, 1996.
15. VILLE F., NELIAS D., *An experimental study on the concentration and shape of dents caused by spherical metallic particles in EHL contacts*, STLE Tribolog Transactions, **42**: 231–240, 1999.
16. WAN G.T.Y., SPIKES H.A., *The behaviour of suspended solid particles in rolling and sliding elastohydrodynamic contacts*, Tribology Transactions, **31**(1): 12–21, 1988.
17. JIN Y., YANG Q., *Ferrographic analysis of wear debris generated in locomotive diesel engines*, Wear, **93**(1): 23–32, 1984.
18. AKAGAKI T., NAKAMURA M., MONZEN T., KAWABATA M., *Analysis of the behaviour of rolling bearings in contaminated oil using some condition monitoring techniques*, Proceedings IMechE, Part J: Journal of Engineering Tribology, **220**(5): 447–453, 2006.
19. PENG Z., KESSISSOGLU N.J., COX M., *A study of the effect of contaminant particles in lubricants using wear debris and vibration condition monitoring*, Wear, **258**: 1651–1662, 2005.
20. KHAN M.A., STARR A.G., COOPPER D., *A methodology for online wear debris morphology and composition analysis*, Proceeding IMechE, Part J: Journal of Engineering Tribology, **222**(J7): 785–796, 2008.
21. SARI M.R., HAIAHEM A., FLAMAND L., *Effect of lubricant contamination on gear wear*, Tribology Letters, **27**: 119–126, 2007.
22. SARI M.R., VILLE F., HAIAHEM A., FLAMAND L., *Effect of lubricant contamination on friction and wear in an EHL contact*, Mechanika, **2**(82): 43–49, 2010.

Received December 13, 2014; accepted version July 5, 2015.
